



## Assessment of pulmonary toxicity of inhaled polycarbonate 3D printer emissions in rats

W. Kyle Mandler, Walter McKinney, Todd A. Stueckle, Alycia K. Knepp, Stacey E. Anderson, Laurel G. Jackson, Sarah Keeley, Kristine Krajnak, A. Parisa Shirzadi, Mariana T. Farcas, Lori Battelli, Sherri A. Friend, Aleksandr B. Stefaniak, Treye A. Thomas, Joanna Matheson & Yong Qian

To cite this article: W. Kyle Mandler, Walter McKinney, Todd A. Stueckle, Alycia K. Knepp, Stacey E. Anderson, Laurel G. Jackson, Sarah Keeley, Kristine Krajnak, A. Parisa Shirzadi, Mariana T. Farcas, Lori Battelli, Sherri A. Friend, Aleksandr B. Stefaniak, Treye A. Thomas, Joanna Matheson & Yong Qian (12 Mar 2025): Assessment of pulmonary toxicity of inhaled polycarbonate 3D printer emissions in rats, Journal of Toxicology and Environmental Health, Part A, DOI: [10.1080/15287394.2025.2473559](https://doi.org/10.1080/15287394.2025.2473559)

To link to this article: <https://doi.org/10.1080/15287394.2025.2473559>



View supplementary material [↗](#)



Published online: 12 Mar 2025.



Submit your article to this journal [↗](#)



Article views: 25



View related articles [↗](#)



View Crossmark data [↗](#)



## Assessment of pulmonary toxicity of inhaled polycarbonate 3D printer emissions in rats

W. Kyle Mandler<sup>a</sup>, Walter McKinney<sup>a</sup>, Todd A. Stueckle<sup>a</sup>, Alycia K. Knepp<sup>a</sup>, Stacey E. Anderson<sup>a</sup>, Laurel G. Jackson<sup>a</sup>, Sarah Keeley<sup>a</sup>, Kristine Krajnak<sup>a</sup>, A. Parisa Shirzadi<sup>a</sup>, Mariana T. Farcas<sup>a</sup>, Lori Battelli<sup>a</sup>, Sherri A. Friend<sup>a</sup>, Aleksandr B. Stefaniak<sup>a</sup>, Treye A. Thomas<sup>b</sup>, Joanna Matheson<sup>b</sup>, and Yong Qian<sup>a</sup>

<sup>a</sup>Pathology and Physiology Branch, Health Effects Laboratory Division, National Institute for Occupational Safety and Health, Morgantown, WV, USA; <sup>b</sup>Office of Hazard Identification and Reduction, U.S. Consumer Product Safety Commission, Rockville, MD, USA

### ABSTRACT

This study investigated the potential pulmonary toxicity of polycarbonate (PC) emissions from fused filament fabrication (FFF) three-dimensional printing (3DP) via inhalation in Sprague Dawley rats. Previously, our results demonstrated no significant pulmonary effects following exposure to a 0.5 mg/m<sup>3</sup> PC. A new exposure apparatus was developed that exposed animals at a concentration of 2.5 mg/m<sup>3</sup>. Sixty rats were randomized into control (filtered air) and exposure groups ( $n = 30/\text{group}$ ). Each group was further divided into five subgroups ( $n = 6/\text{subgroup}$ ) with exposure durations of 1, 4, 8, 15, or 30 days (4 hr/day, 4 days/week). Following a 24-hr post-exposure period, body weight was measured, and blood samples were collected for hematological and biochemical analysis. Bronchoalveolar lavage fluid (BALF) was obtained from the right lung for cytology. The left lung and head/nasal tissues were preserved for histopathological evaluation. Lung deposition was estimated using the Multiple-Path Particle Dosimetry model, electron microscopy, and enhanced darkfield microscopy. In addition, filter samples were collected to measure bisphenol A. Exposure resulted in an estimated deposition of 0.28  $\mu\text{g}/\text{day}$  within the alveoli and small airways. Microscopy indicated limited evidence of macrophage uptake. No significant changes were observed in BALF cell counts, lactate dehydrogenase activity, or hematological parameters. BALF levels of tissue inhibitor of metalloproteinases-1 and protein were elevated in the 30-day exposure group, although histopathology revealed no exposure-related changes in the lungs. In conclusion, this study found no marked pulmonary inflammation or toxicity in rats exposed to 2.5 mg/m<sup>3</sup> of PC 3D printing emissions for up to 30 days (4 hr/day).



### Keywords


3D printing; inhalation; bisphenol A; microplastics and nanoplastics; VOC

## Introduction

Three-dimensional printing (3DP), a type of material extrusion additive manufacturing, is a process of creating a three-dimensional object from a digital model by building up the object layer by layer, using a variety of materials such as plastics, metals, ceramics, and even food. 3DP has revolutionized many industries, including manufacturing, medicine, and education. 3DP is also becoming increasingly popular for personal use, with many individuals using it to create custom objects for their homes and businesses. The growth of 3DP in the next decade is expected to be rapid, with the global size of the industry projected to reach \$37.2 billion (Placek 2023). Fused filament fabrication (FFF) is the most common type of

material extrusion 3DP. FFF 3DP builds objects by extruding a heated thermoplastic filament through a nozzle to layer material on a print bed along a path defined by the digital model. FFF printers are relatively inexpensive and easy to use, making them popular for hobbyists and small businesses. There currently exist several types of filaments for FFF 3DP, including polylactic acid, polyethylene terephthalate glycol, thermoplastic polyurethane, nylon, acrylonitrile butadiene styrene (ABS), and polycarbonate (PC). Each of these materials may contain dyes, pigments, metals (Tedla et al. 2022), or nanomaterials to achieve the aesthetic or mechanical properties desired by the consumer (Tedla and Rogers 2023; Zarybnická et al. 2022). The widespread adoption of 3DP has

**CONTACT** W. Kyle Mandler  [oe11@cdc.gov](mailto:oe11@cdc.gov)  Pathology and Physiology Branch, Health Effects Laboratory Division, National Institute for Occupational Safety and Health, 1095 Willowdale Road, Morgantown, WV 26505, USA

 Supplemental data for this article can be accessed online at <https://doi.org/10.1080/15287394.2025.2473559>

This work was authored as part of the Contributor's official duties as an Employee of the United States Government and is therefore a work of the United States Government. In accordance with 17 U.S.C. 105, no copyright protection is available for such works under U.S. Law.

raised concerns regarding potential adverse health risks associated with inhaled emissions. These emissions include ultrafine particles (UFPs) (Yi et al. 2016), with diameters less than 100 nanometers, which can penetrate deep into the lungs (Oberdörster 2000). UFPs have been linked to a number of health problems, including respiratory illness (MacNee and Donaldson 2003; Peters et al. 1997), cancer (Liao et al. 2011), and altered vascular function (Mandler et al. 2017, 2018). Further, FFF releases gases, including volatile organic compounds (VOCs) from heated filaments (Davis et al. 2019; Stefaniak et al. 2019). VOCs are organic chemicals with high vapor pressure at room temperature, and some, like benzene (Cronkite et al. 1989), formaldehyde (Swenberg et al. 2013), and styrene, are known to be pulmonary toxicants (Bus et al. 2024). Inhalation is the primary exposure route for VOCs, although dermal and ingestion pathways also exist (Feld-Cook and Weisel 2021).

Previous investigators demonstrated pulmonary toxicity attributed to FFF 3DP to emissions using both *in vitro* and *in vivo* methods (M. Farcas et al. 2024; M. T. Farcas et al. 2019, 2020). In the *in vitro* studies, human small airway epithelial cells were exposed to emissions collected from ABS and PC filaments in a custom-designed 3DP emission characterization chamber. After 24 hr incubation with this conditioned media, PC emissions displayed greater cytotoxicity compared to ABS, inducing oxidative stress, apoptosis, and necrosis in the cells. Further, exposure triggered the release of pro-inflammatory cytokines (IL-12p70, IL-13, IL-16, IL-1 $\beta$ , IL-1 $\alpha$ , IL-6, IL-8, and TNF- $\alpha$ ) (M. T. Farcas et al. 2019). To translate the *in vitro* findings into a whole-body model, rats were exposed to PC printing emissions via inhalation (M. Farcas et al. 2024). A novel exposure system was designed to collect emissions from three synchronized 3D printers and deliver them to a characterization chamber before reaching the inhalation chamber. Our prior *in vivo* studies employed an exposure regimen: 4 hr/day, 4 days/week for 1, 4, 8, 15, or 30 days at an average concentration of 0.529 mg/m<sup>3</sup> with a mean electrical mobility diameter of 40 nm. In addition to particulates, several VOCs were detected in the emissions, including phenol, acetaldehyde, acetone, ethanol, and ethylbenzene. Bisphenol A (BPA) was

measured at  $5.3 \pm 0.18 \mu\text{g}/\text{m}^3$ . Pulmonary toxicity was assessed using histopathology and a comprehensive panel of biomarkers, including protein and enzyme activity in bronchoalveolar lavage fluid (BALF), cell counts, hematological parameters, and blood markers of organ function. Despite the observed cytotoxicity *in vitro*, our *in vivo* exposure at this concentration resulted in only transient changes in a few biomarkers and no histopathological alterations (M. Farcas et al. 2024).

The incongruity between our *in vitro* and *in vivo* results might be due in large part to the much lower total particle mass deposition achieved during the *in vivo* exposure. In M. T. Farcas et al. (2019) an average particle deposition of 0.424  $\mu\text{g}/\text{cm}^2$  of well surface was achieved, while in M. Farcas et al. (2024), the lung deposition was estimated at 0.0152  $\mu\text{g}/\text{cm}^2$  of alveolar surface, an almost 28-fold difference. Our principal objective in the present study was to redesign the exposure system to increase the exposure mass concentration of PC emissions to an occupationally relevant level (2.5  $\mu\text{g}/\text{m}^3$ ) in an *in vivo* experiment. This exposure concentration falls within workplace measurements recorded during 3D printing with PC filaments m<sup>3</sup> (Chýlek et al. 2019; McDonnell et al. 2016; Runström et al. 2022). It was postulated that increasing the exposure mass concentration of PC emissions may lead to observable pulmonary toxicity in rats. The study results might aid to clarify the potential adverse health risks of exposure to FFF 3D printing emissions by providing a more accurate assessment of the *in vivo* effects of inhaled particles. This information may be used to inform the development of safety guidelines for 3D printing users.

## Methods

### Three-dimensional printer emissions inhalation exposure system

An inhalation exposure system was specifically designed and constructed to deliver a high concentration of FFF 3DP emissions to a whole-body rodent exposure chamber. This system was a modified version of a previously described system (M. Farcas et al. 2024). The new system and

the older system both automatically controlled chamber pressure, air flow, temperature, particle concentration, and exposure time using custom software. The modification from the old system was made by removing the three 3D printers from the generation chamber and replacing them with five 3D printer extruders (Titan Aero 0.6 mm nozzle, E3D, Oxfordshire UK) and custom fume collectors. A diagram of the print head and labeled picture of this setup are illustrated in Supplemental Figures S1 and S2. This method of generating 3D printer emissions does not involve printing solid parts; it simply extrudes the filament into air and collects the fume at the nozzle. Dunn et al. (2020) previously noted that over 98% of emissions during 3DP is generated at the printer nozzle.

A rendering of one of the 3D printer extruders with custom fume extractor used in this study is depicted in Supplemental Figure S3. The extractor was made from 304 stainless steel. The square section of the part was 23 × 23 × 10 mm in size, and the circular cavity was 16 mm in diameter. The inner diameter and outer diameter of the tubing port was 6 mm and 9 mm, respectively. Five liters per minute of air flowed through each extractor, for a total of 25 L/min for all five nozzles, and into the exposure chamber. Conductive silicon tubing (TSI Inc., Shoreview, MN) was used to connect all five nozzles to a 6-way stainless steel manifold. The sixth port exited the generator chamber and led to the top of the exposure chamber using conductive tubing.

To ensure consistent and reliable emission generation, it was decided to remove the 3DP function from the exposure system. Utilizing the older system for part printing introduced several potential inconsistencies. Detachment of the part from the build plate might lead to print failure and disrupt emissions generation. Upward warping of the part might result in nozzle clogging due to reduced nozzle-part distance. In addition, occasional failures in the automatic bed/nozzle leveling system would prevent printing altogether. To address these limitations and achieve higher exposure concentrations, the 3D printers were replaced with five individual 3D printer extruders equipped with fume collectors.

### **Three-dimensional printer settings for PC filament**

Polycarbonate is a higher-temperature material than most other plastic filaments (useful working temperature for objects might be as high as 150°C). The manufacturer suggested that the temperature range for the filament to be 260–310°C, with higher temperatures yielding a faster print and better layer adhesion. The 5 FFF 3D printer extruders were each programmed to operate simultaneously at 300°C with an extrusion rate of 60 g/h using commercially available black 2.85 mm PC filament (Manufacturer 1). A brass nozzle with diameter of 0.6 mm was installed on all extruders. When not in use, the filament was stored at room temperature in an airtight dry box. An extrusion rate of 60 g/h is in the typical range for printing PC parts with a 0.6 mm nozzle.

### **Three-dimensional printing with PC emissions collection and characterization**

3DP emissions were collected and characterized using a variety of well-established methods, including continuous aerosol mass monitoring, particle count, and size analysis, VOCs sampling, and VOCs analysis. This comprehensive approach provides confidence in the accuracy and reliability of the results. Specifically, a Data RAM (DR-40000 Thermo Electron Co., Franklin, MA) and gravimetric determinations (37 mm cassettes with 0.45 µm pore-size Teflon filters, 1 L/min sample flow) were used to calibrate and verify the Data RAM readings during each exposure run. For this study, a 4-h average concentration of 2.5 mg/m<sup>3</sup> was the daily target. An Electrical Low-Pressure Impactor (ELPI Classic, Dekati Technologies, Finland) was used to collect count-based particle aerodynamic diameter size distribution data. A mobility particle sizer (SMPS, Model 3081, TSI Inc. Shoreview, MN) was employed to collect count-based electric mobility particle size distribution data, and a cascade impactor utilized to collect mass-based aerodynamic diameter size data (MOUDI 110 R, TSI Inc. Shoreview, MN). All particle sizing samples were conducted in the same manner as a typical exposure run but without animals present in the exposure chamber.



BPA and BPA diglycidyl ether were measured using OSHA method 1018 (Occupational, Health, and Pearce). The time integrated samples were collected on glass fiber filters (SKC 225–709 Lot # 21600-7E5-274). Each sample filter was placed in a separate glass test tube. Each sample cassette was wiped separately using a glass fiber filter wetted with 100  $\mu$ l of ethanol. The wipes were placed in separate glass test tubes. Sample filters and wipes were extracted in 3 ml of acetonitrile and then placed on a mechanical flatbed shaker for 30 min. A portion of each was then transferred to individual auto-sampler vials for analysis using HPLC (Vanquish UHPLC, Thermo Fisher, Waltham, MA) with ultraviolet detection.

Phenol and cresols were measured using OSHA method 32 (Occupational, Health, and Cummins). The time integrated samples were collected on XAD-7 sorbent tubes (SKC 226–95, lot#14285). The sorbent was removed from each tube and placed into separate test tubes. The glass wool from the front section and middle glass wool plug were added to the front sorbent section. The back sorbent section was placed in a separate test tube. The samples were then chemically desorbed using 2 ml methanol. The samples were capped and placed on a mechanical shaker for 30 min. After desorption, the samples were hand shaken and an aliquot of each was immediately transferred to autosampler vials and analyzed via HPLC.

## Animals

Male Sprague-Dawley (SD) rats (6–7 weeks old, 200–225 g) were purchased from Hilltop Lab Animals and housed in ventilated polycarbonate cages, 4 rats per cage. The rats were acclimated for at least 7 days before the start of the study. The facility provided a controlled environment with HEPA-filtered air, a temperature of  $22 \pm 2^\circ\text{C}$ , and a humidity of 40–60%. The rats were fed irradiated Teklad 2918 diet and provided with ALPHA-dri®/Teklad sani-chips bedding mix and tap water *ad libitum*. The study protocol was reviewed and approved by the CDC-Morgantown Institutional Animal Care and Use Committee. The CDC-Morgantown animal care and use program is accredited by AAALAC International.

## Experimental design

Sixty male SD rats were randomly assigned to either an air control group or a 3DP emissions-exposed group, with six rats per subgroup allocated to each exposure duration (1, 4, 8, 15, or 30 days). The air control group inhaled the HEPA-filtered air for 4 hr per day, 4 days per week. The 3D printer emission-exposed group inhaled real-time emissions from FFF 3DP with PC filament for the same duration and frequency. Twenty-four hours after the final exposure, rats were euthanized by intraperitoneal injection of pentobarbital. Body weight was measured, and blood was collected from the abdominal aorta for hematological and biochemical analysis. BALF was collected from the right lung. The heart and lungs were collected and stored at  $-80^\circ\text{C}$  for further analysis (e.g., gene expression, protein analysis). The left lung and head/nasal tissues were preserved in formalin for histopathological evaluation.

### *Three-dimensional PC filament emission particle deposition estimates in the nasal passages, tracheobronchial, and alveolar regions*

The Multiple-Path Particle Dosimetry (MPPD) model (Anjilvel and Asgharian 1995) was used to estimate PC emission particle deposition mass for the rat head/nose, tracheobronchial, alveolar regions, and collective deposition for tracheobronchial and alveolar regions. Parameters used for deposition calculations can be found in Supplemental Table S1. A mass median aerodynamic diameter of 78 nm was used in the MPPD model because of the MOUDI measurement results. There was not sufficient resolution on the lower stages of the MOUDI to determine an accurate geometric standard deviation so a value of 1 (the default for a long normal distribution) was used. The particle mass density was set to  $1.2 \text{ g/cm}^3$  for the MPPD model as an estimate because this is the density of the PC filament.

## BALF analysis

### *BALF collection and cytology*

Three ml cold PBS was passed into the right lung via a tracheal cannula; the lung was massaged for

30 sec, the cold PBS was withdrawn, and the process was repeated a second time, yielding the first fraction of BALF. A second BALF fraction was collected by repeating the aforementioned process using 3 ml aliquots of PBS until a 9 mL volume was recovered. The two BALF fractions were centrifuged ( $800 \times g$ , 10 min, 4 °C), and the supernatant from fraction one and the cell pellets from both fractions were kept for further analysis (supernatant from fraction two was discarded). The supernatant was used to measure total protein levels, lactate dehydrogenase (LDH) activity, and cytokine levels. The pellets were combined, resuspended in 1 mL PBS (Lonza, Pearland, TX) and used for a total cell count and cell differential (Beckman Coulter Multisizer 4 particle counter, Coulter Electronics, Hialeah, FL).

#### ***Transmission electron microscopy (TEM) staining of BALF cells***

BALF cells were initially fixed in 1 ml of Karnovsky's fixative (containing 2.5% glutaraldehyde and 3.4% paraformaldehyde in 0.1 M sodium cacodylate buffer) for optimal preservation. After fixation, the cells were stored at 4°C until further processing. To enhance the cellular contrast, postfixation was performed with 2% osmium tetroxide for 1 hr. Subsequently, the samples underwent mordanting with 1% tannic acid, followed by *en bloc* staining with 0.5% uranyl acetate for improved membrane contrast. Dehydration was achieved through a graded ethanol series, followed by infiltration with propylene oxide. Finally, the samples were embedded in EPON™ (epoxy resin) to polymerize blocks for sectioning. Ultrathin sections (70 nm) were generated from the embedded blocks and placed on grids. To further enhance the contrast for TEM imaging, these sections were double stained with 4% uranyl acetate and Reynold's lead citrate. The stained sections were then visualized using a JEOL 1400 transmission electron microscope (JEOL, Tokyo, Japan).

#### ***BALF total protein and lactate dehydrogenase (LDH) activity***

A Pierce™ BCA Protein Assay Kit (Fisher Scientific) and an LDH Reagent Set (Pointe Scientific, Lincoln Park, MI) were used according to manufacturer's instructions in conjunction with a Synergy H1

Microplate Reader (BioTek, Winooski, VT) to collect total protein (562 nm) and LDH activity (340 nm) data, respectively, from the BALF samples.

#### ***BALF cytokine levels***

V-PLEX Pro-inflammatory Panels 1 & 2 Rat Kit (MSD, Rockville, MD) was used in conjunction with a QuickPlex SQ 120 plate reader (MSD, Rockville, MD) to collect pro- and anti-inflammatory cytokines data from the BALF samples. Analytes measured were: NGAL1, TSP-1, TIMP-1, MCP-1, IFN- $\gamma$ , IL-1 $\beta$ , IL-4, IL-5, IL-6, IL-10, IL-13, KC/GRO, and TNF- $\alpha$ .

#### ***Blood processing and analysis***

Blood collected in EDTA-containing and clot-activator-/polymer gel-containing vacutainers was processed and analyzed as previously described in M. T. Farcas et al. (2020).

#### ***Characterization of blood cells and hematological parameters***

A complete blood count was performed for each sample 30–45 min after collection using a ProCyt Dx Hematology Analyzer (IDEXX Laboratories, Inc., Westbrook, ME).

#### ***Lung and nasal passages histopathological evaluation***

The unlavaged left lung was inflated with 10% neutral buffered formalin (NBF), embedded in paraffin, cut at 5  $\mu$ m on Schott slides, and stained with Hematoxylin and Eosin (H&E) for histopathological evaluation. Lesions were reviewed by a board-certified veterinary pathologist and classified in the following manner: WNL = within normal limits; 1 = minimal change (barely exceeds WNL); 2 = mild/slight change (lesion is identifiable but is of limited severity); 3 = moderate change (lesion is prominent with a potential for increased severity); 4 = severe change (lesion occupies the majority of the organ and is as severe as possible). After processing the lungs, the nasopharynx was lightly flushed with 10% NBF, and the nasal passages were collected. Nasal tissues were fixed in formalin for 1 week, then decalcified in 13% formic acid. Standard nasal sections (T1, T2, T3, and T4) were taken (Young 1981) and embedded in paraffin, cut at 5  $\mu$ m, and stained with H&E.

### Enhanced darkfield microscopy

To ascertain PC particle deposition in the lower airways and deep lung, separate H&E and trichrome stained lung sections cut from paraffin blocks were evaluated with enhanced darkfield microscopy on a CytoViva system (Auburn, AL) as described by Stueckle et al. (2018). Air-only and PC exposed lung sections from Day 1 and Day 30 animals ( $n = 6$ ) were evaluated to assess acute deposition and highest estimated deposition following exposure, respectively. Evaluation of nasal passages and collected BALF cytopins was also performed on Day 1 animals to confirm 3D particle inhalation and macrophage phagocytosis ability. Representative digital images of ciliated airways, terminal bronchiole, bronchioalveolar duct, and alveoli at 20–100 $\times$  magnification were acquired using an Olympus D73 camera on an Olympus BX41 microscope. 60 $\times$  or 100 $\times$  oil immersion objectives were used for high-quality imaging and hyperspectral scans. Background nano-sized silica particles, byproduct of glass slide handling, were identified in air-only exposed tissues and not considered in PC-exposed lung sections. Suspected PC particles and agglomerates co-localized with tissue and within the tissue focal plane were imaged under different intensities of light to ascertain primary particle and agglomerate morphology. Hyperspectral scans using CytoViva integrated spectrograph, digital camera, and ENVI v4.8 software were acquired of trichrome stained slides to compare spectra of PC particles to nanosilica and other nanosized (<100 nm) particles in air control tissue.

### Statistical analysis

All statistical analyses were performed using SAS/STAT v9.4 for Windows with a  $p$ -value <0.05. Two-way variance analyses (treatment  $\times$  duration) were performed on the measured variables. Post hoc comparisons between relevant groups were performed using Fisher's LSD. All errors are reported as standard deviations.

## Results

### Emissions characterization

The average mass concentration determined with gravimetric filters over all exposure days in this study was 2.42 mg/m<sup>3</sup> with a standard deviation of

0.3 mg/m<sup>3</sup>. The gravimetric filter measurements serve as more accurate measurements of mass concentration and were used to verify our direct reading instrument. The average aerodynamic size distribution plot (particle count based) of the PC-emissions inside the exposure chamber measured with the ELPI during a test run is shown in Figure 1(a). The average aerodynamic size distribution plot (mass based) of the PC emissions inside the exposure chamber measured with the MOUDI is shown in Figure 1(b). The smallest stage (27 nm or less) of the ELPI registered the highest particle counts. Figure 1(c) illustrates the data from the SMPS during a test run. The mean particle electric mobility diameter was 63 nm. Most of the particle mass was on the smallest impactor stage, which means the MMAD was 78 nm or less. Higher resolution versions of each panel from Figure 1 may be found in Supplemental Figures S4, S5, and S6. The average BPA concentration was measured at  $78.3 \pm 5.42$   $\mu$ g/m<sup>3</sup> (limit of detection (LOD) = 0.2  $\mu$ g, lower limit of quantification (LLOQ) = 0.67  $\mu$ g). Phenol (LOD = 0.4  $\mu$ g, LLOQ = 1.3  $\mu$ g), cresol (LOD = 0.4  $\mu$ g, LLOQ = 1.3  $\mu$ g), and Diglycidyl Ether (LOD = 0.1  $\mu$ g, LLOQ = 0.33  $\mu$ g) were not detected in any sample.

### MPPD modeling

Modeling estimates for the 3DP particle deposition suggest that 86.28  $\mu$ g was deposited per day in the head and nose, 6.41  $\mu$ g in the tracheobronchial region, and 8.29  $\mu$ g in the alveolar region (Table 1). Estimated BPA deposition per day was 0.175  $\mu$ g in the nose, 0.075  $\mu$ g in the tracheobronchial region, 0.354  $\mu$ g in the lung, and 0.279  $\mu$ g in the alveolar region, with a total daily deposition of 0.529  $\mu$ g (Table 2). These calculations assume that the BPA concentration is uniform across particle sizes.

### Body weight

Body weight values were not markedly different from control at any given timepoint except for Day 15, when the 3DP group weight averaged  $389.09 \pm 22.445$  g, vs  $360.97 \pm 17.679$  g for control Figure 2(a).

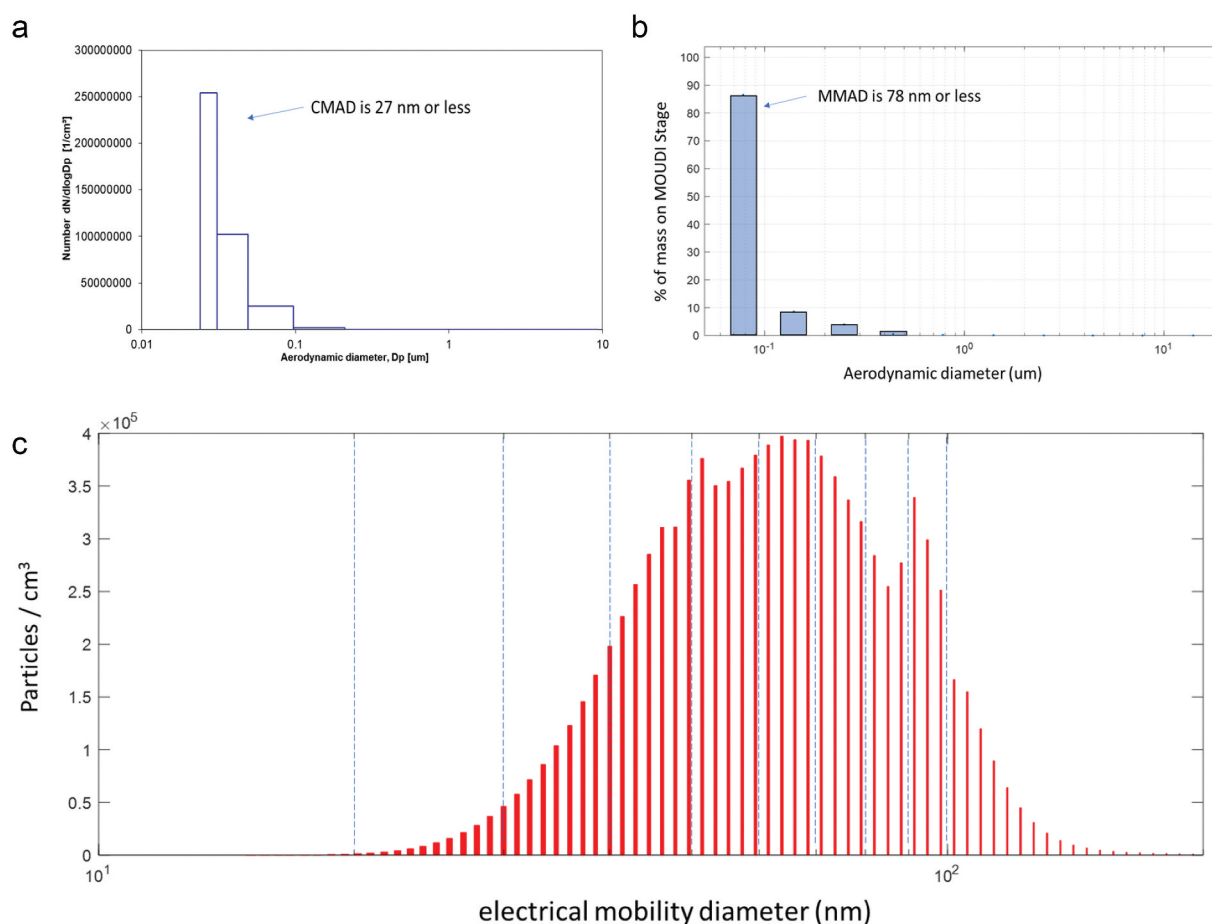


**Figure 1.** Real-time particle size characterization. a) ELPI b) MOUDI, c) SMPS. The average mass concentration determined with gravimetric filters over all exposure days in this study was  $2.42 \text{ mg/m}^3 \pm 0.3 \text{ mg/m}^3$ . The smallest stage (27 nm or less) of the ELPI registered the highest particle counts. The mean particle electric mobility diameter was 63 nm. Most of the particle mass was on the smallest impactor, meaning the MMAD was 78 nm or less.

**Table 1.** MPPD Modeling Estimated 3DP Particle Deposition

Days of exposure					
Deposition Region ( $\mu\text{g}$ )	1	4	8	15	30
Head and Nose	86.28	345.12	690.24	1294.2	2588.4
Tracheobroncheolar	6.408	25.632	51.264	96.12	192.24
Alveolar	8.2896	33.158	66.316	124.34	248.69

**Table 2.** MPPD Modeling Estimated BPA Deposition

Estimated BPA deposition ( $\mu\text{g}$ )					
	Nose	Tracheo	Alveolar	Lung	Total
1d	0.181	0.082	0.28	0.351	0.534
4d	0.704	0.302	1.11	1.41	2.11
8d	1.41	0.6	2.23	2.82	4.21
15d	2.64	1.12	4.17	5.29	7.92
30d	5.29	2.25	8.33	10.6	15.8

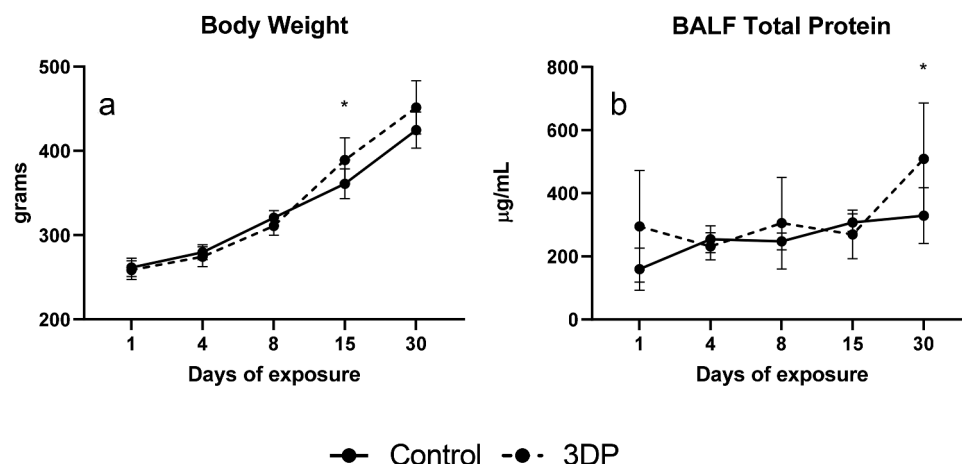


**Figure 2.** a) bodyweight was increased in 3DP group at day 15 compared to control. b) BALF total protein was increased in 3DP group at day 30. \* indicates significant difference from control ( $p < 0.05$ ). Values represent mean  $\pm$  SD.

### BALF total protein

BALF total protein values were not markedly different from control at any given timepoint except for Day 30, when the 3DP group averaged  $509.21 \pm 177.42$   $\mu\text{g/mL}$  vs.  $329.24 \pm 88.504$   $\mu\text{g/mL}$  for control Figure 2(b).

### BALF LDH

No significant differences among treatment groups at any timepoint were observed in mean BALF LDH activity (data not shown).

### BALF cell differential

No marked differences in the BALF cell count differential among treatment groups were observed for macrophages, polymorphonuclear leukocytes (PMN), lymphocytes, or eosinophils (Figure 3).

### BALF cell TEM

Suspected particle uptake in macrophages was observed after 30 days of exposure, with similar patterns seen at all post-exposure durations. Particles were localized within membrane-lined vacuoles as indicated by the white arrow in Figure 4. Notably, no significant alterations in overall BALF cell morphology were detected by TEM analysis.

### BALF cytokines

IFN- $\gamma$ , IL-1 $\beta$ , IL-4, IL-5, IL-6, IL-10, IL-13, TSP-1, and TNF- $\alpha$  were not detected in quantifiable levels in the BALF of either exposed or control animals. TIMP-1 was increased to  $153.23 \pm 36.13\%$  of control after 30 days of exposure in the 3DP group. NGAL1, MCP1, and KC/GRO were not markedly different among treatment groups at any time point (Figure 5).

### Hematology

Eosinophil % was elevated in the exposed group at day 30. No other significant changes in any parameter were noted (Supplemental Table S2).

### Histopathology

H&E-stained sections of left lung (LL) were examined under a microscope for evidence of test article deposition and for the presence of test-article associated pathology. Rats exposed to HEPA-filtered air were employed as controls. Microscopic evidence of test article-associated pathology was not observed in any sections of the lung examined from exposed rats.

### Enhanced darkfield microscopy

Day 1 and Day 30 air control tissues exhibited occasional presence of nanosized silica particulate from slide handling, no adverse pathology,



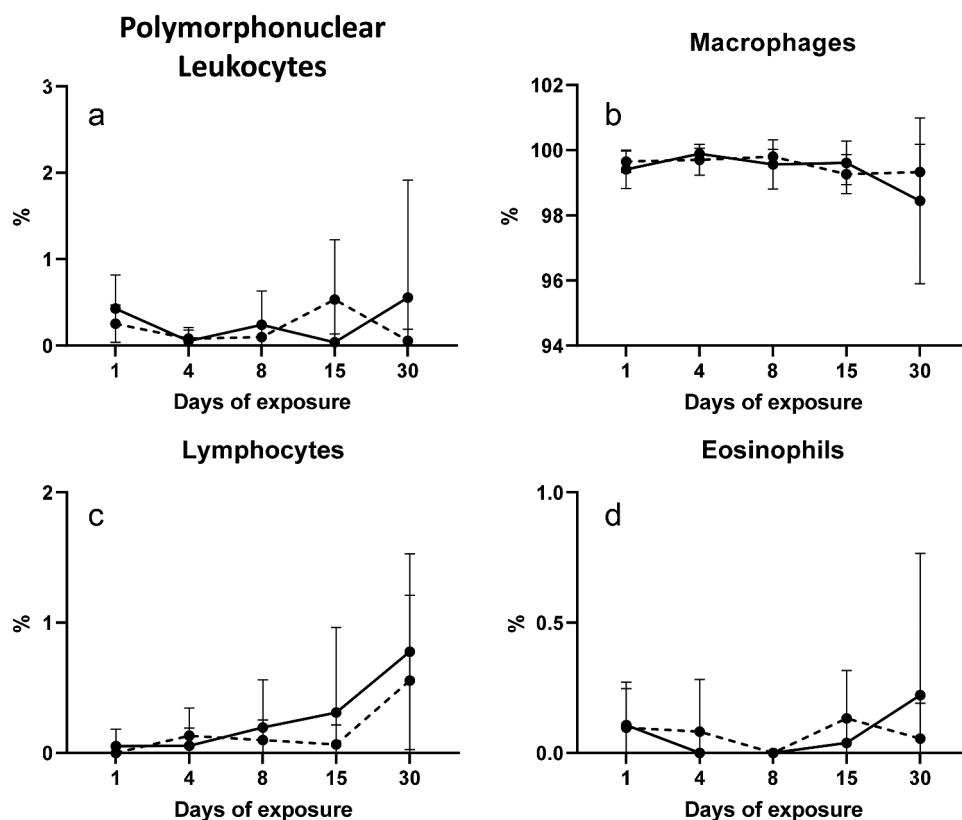


**Figure 3.** BALF cell differential. No differences were noted in any cell type for at any timepoint. Values represent mean  $\pm$  SD.

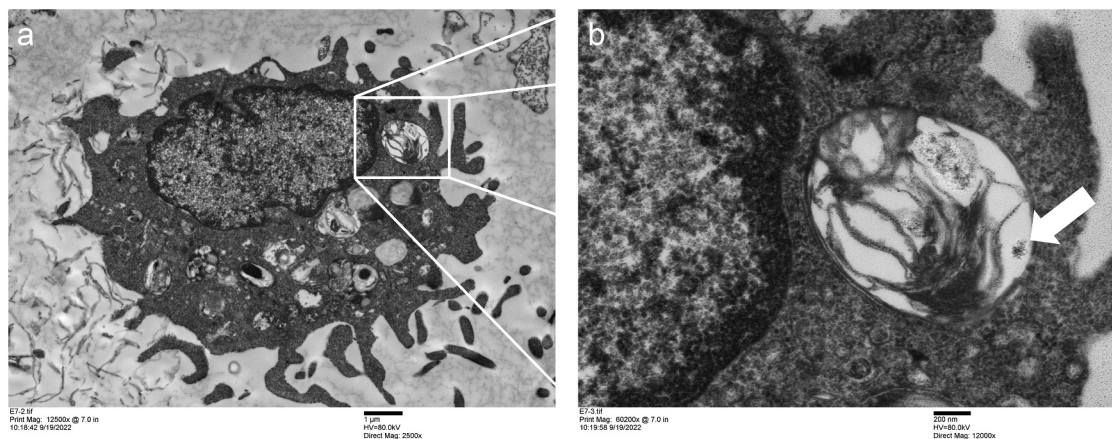


**Figure 4.** Transmission electron micrographs of BALF macrophage (a). Arrow in inset (b) indicates suspected 3DP particle agglomerate in vesicle. Scale bars indicate size.

particle-free resident macrophages, and no signs of PMNs (Figure 6). Nanosized silica, a byproduct of slide processing, exhibited a visible white scattered light spectrum with peak wavelength intensity approaching near-red at  $675 \pm 20$  nm (Figures 7 and 8). PC-exposed Day 1 tissues displayed little to no evidence of suspected PC particles in alveoli, ciliated airways, or macrophages. One or two small

agglomerates of suspected PC were found per tissue section. Two particle-laden macrophages were found in one animal with particle hyperspectral matching that of suspected PC particle (Figure 7). Suspected submicron and ultrafine PC particles were found deposited or impacted in nasal cavity epithelium in Day 1 animals (Figure 9). Macrophages in collected BAL cytopins in Day 1

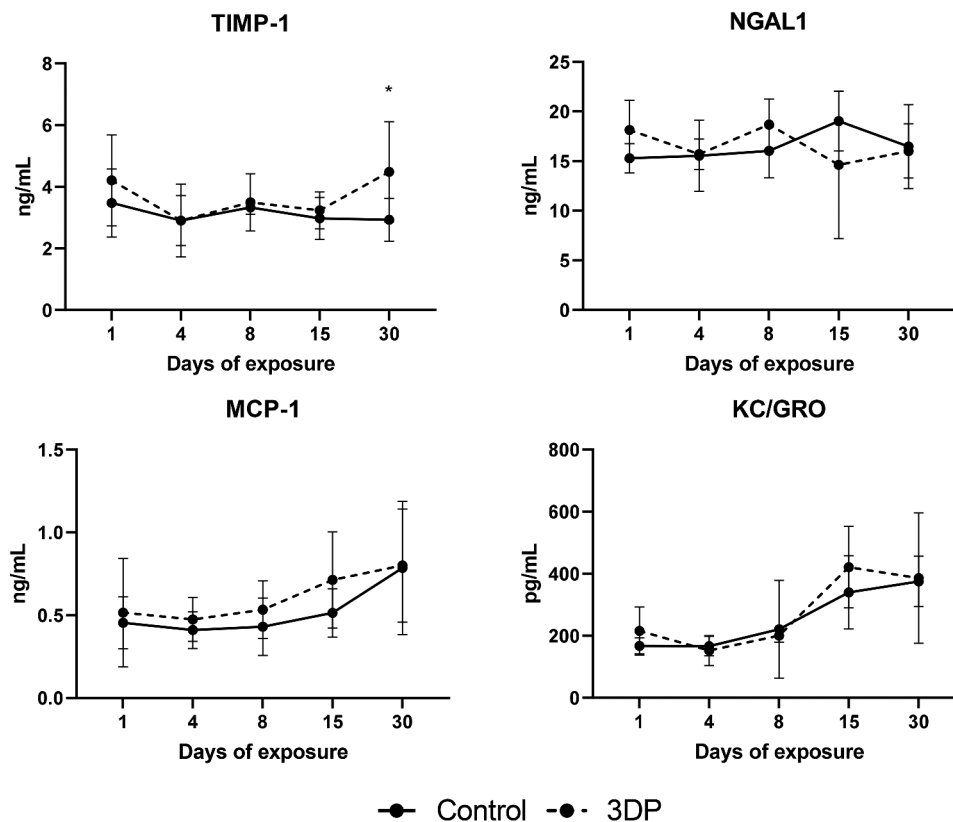


**Figure 5.** BALF inflammatory cytokines. TIMP-1 (a) was elevated ( $p < 0.05$ ) compared to control at day 30. Values ng/mL ng/mL represent mean  $\pm$  SD.

animals showed minimal uptake of suspected PC particles (Figure 9). Conversely, Day 30 tissues exhibited suspected PC particles as submicron- or micron-sized agglomerates co-localized with the alveoli (Figure 8). Primary particles exhibited a yellow visible scattered light spectrum and irregular, low aspect rounded morphology. Agglomerates consisted of doublets of primary particles in airspaces or on alveolar surface to 10 s or 100 s of particles deposited on the alveolar surface. Hyperspectral analysis of the suspected PC revealed scattered light spectra shifted to the left in the visible spectrum, compared to nanosilica (fragments from slide cutting), with a mean peak intensity of  $615 \pm 7.2$  nm. One animal displayed a PC particle-laden macrophage present in the ciliated airway (Figure 6). PC particles were occasionally found in the ciliated airway, terminal bronchiole, or bronchioalveolar duct. Finally, suspected PC particles were found to be co-localized in a blood vessel ( $n = 2$  of 6 animals) near large agglomerates in an alveolus (Figure 6), thus suggesting the deposited PC particles might

translocate from the deep lung airspace into the circulatory system.

## Discussion

The exposure system used in our prior study employing three consumer-grade 3D printers was only able to achieve a maximum inhalable PC concentration of  $0.529 \text{ mg/m}^3$ . To achieve a near 5-fold rise in aerosol concentration to bridge the delivered dose gap with our *in vitro* findings, the system was redesigned with five print heads for continuous filament extrusion. This greater exposure resulted in estimated total alveolar depositions of  $8.28 \mu\text{g}$ ,  $33.15 \mu\text{g}$ ,  $66.31 \mu\text{g}$ ,  $124.34 \mu\text{g}$ , and  $248.69 \mu\text{g}$  at the 1, 7, 15, and 30 days of exposure, respectively (Table 1). Particle size and morphology of suspected PC particulate in rat lung sections were consistent with particle characterization in this study and a previous study by our group (M. Farcas et al. 2024). To date, most process-derived micro- and nanoplastic particles (MNP) found in the respiratory system are  $1730 \text{ nm}$  (Feng et al. 2023). Particles

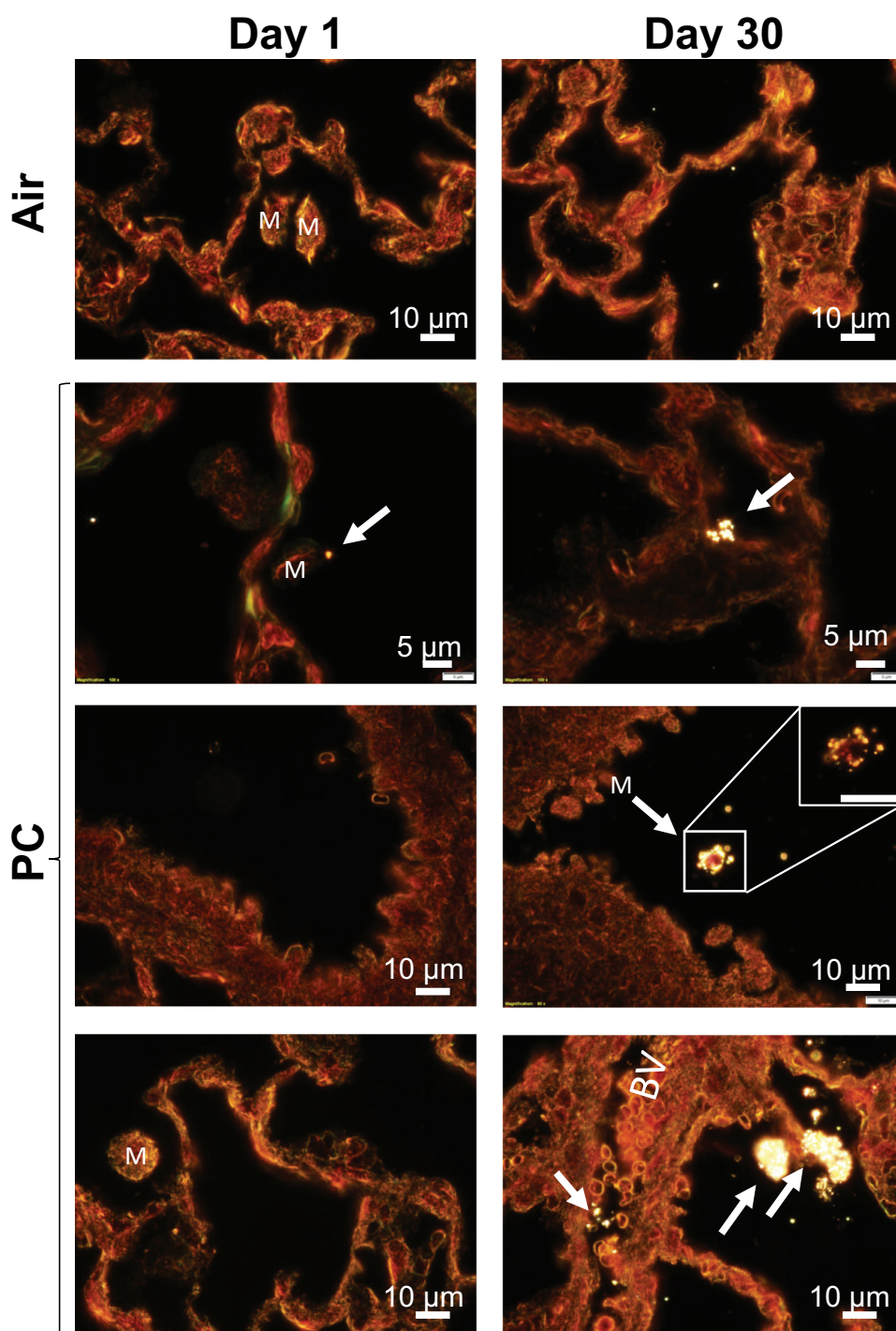


**Figure 6.** Darkfield enhanced microscopy of polycarbonate (PC) nanoparticulate deposition in rat lung following inhalation exposure to 3D PC printer filament. Air-only exposed lungs showed only signs of incidental nanosized silica from glass slide handling with no signs of suspected nanoplatic particulate. Suspected PC particulate (white arrows) rarely appeared in the alveoli of Day 1 animals. PC agglomerates were found primarily deposited in alveoli, with some evidence in a macrophage (M) in the ciliated airway and nearby blood vessel (BV). Images were taken at 60 and 100× magnification. Scale bars report size.

in the submicron range to single micron range deposit in the airway and deep lung with clearance via mucous ciliary escalator and recognized and cleared by alveolar macrophages. Submicron and

ultrafine particles (<100 nm) can deposit in the deep lung, potentially escape macrophage detection, and experience translocation and extrapulmonary transport (Geiser 2002). Indeed, our data indicate

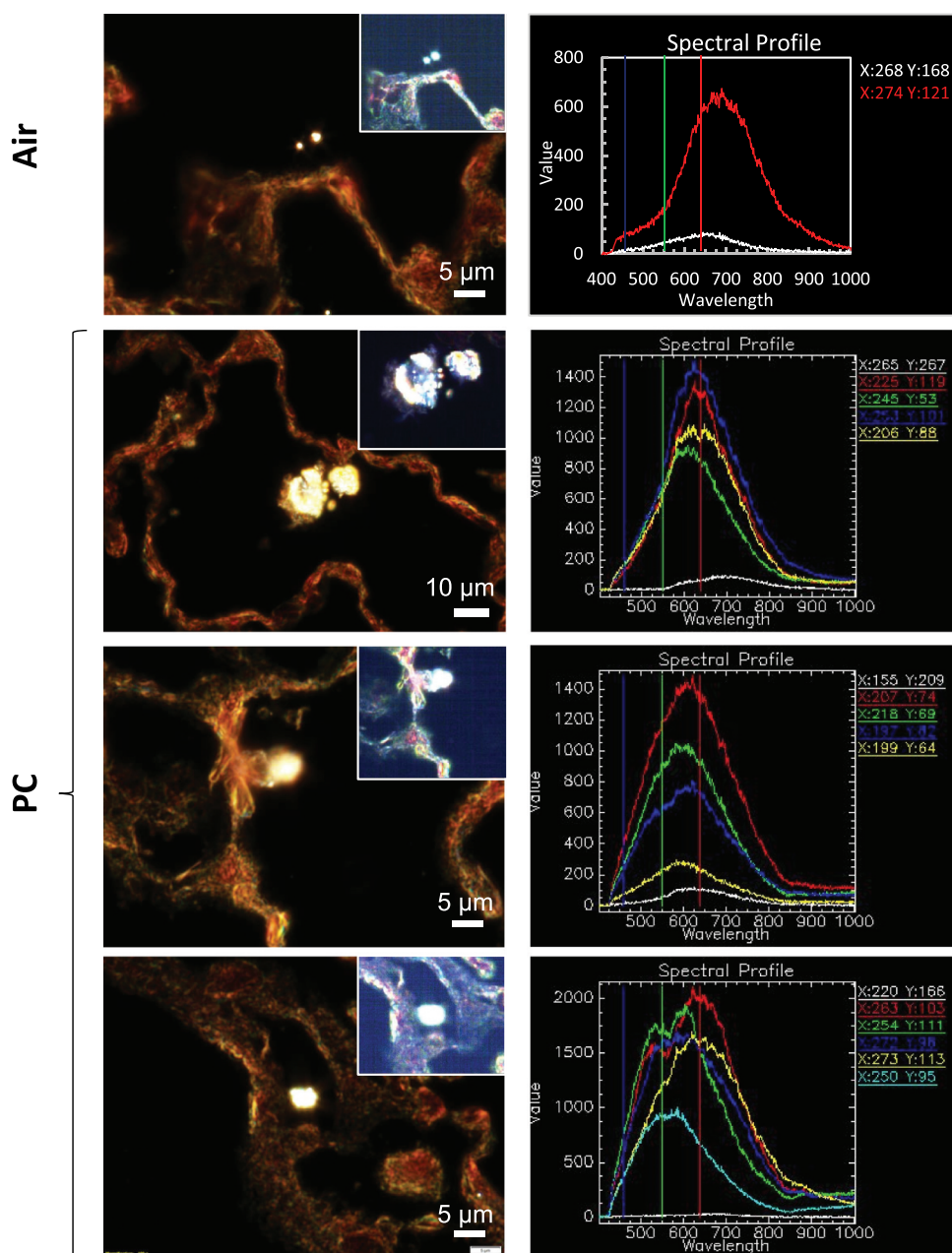


**Figure 7.** Hyperspectral imaging of nanosized particulate in rat lung following 1 day of PC emission exposure. Nanosilica (red box) from glass slides was found throughout all X-sections. Suspected PC particles (blue box) were found deposited in alveoli, ciliated airway, and blood vessels.

that a fraction of the particles is able to translocate into pulmonary blood vessels (Figure 8). The presence of PC agglomerates in Day 30 alveoli with limited evidence of macrophage phagocytosis suggests that inhalation of 3DP PC aerosols followed by deposition of PC UFPs in the lung evades the lung's primary particle defense system. Given that the daily mass and particle count deposition were low compared to bolus exposure studies and that little deposited PC particle was found after 1 day of exposure in

the lungs, it is reasonable to conclude that particle load and size were not sufficiently high to elicit a macrophage phagocytosis response. Accumulation of agglomerates in alveoli and the alveolar surface over a 30-day period might go unrecognized. This might subsequently lead to translocation of PC particle through the air-blood barrier to the blood circulatory system (Kreyling et al. 2014; Nemmar et al. 2002) and extrapulmonary transport to other sensitive tissues with high density



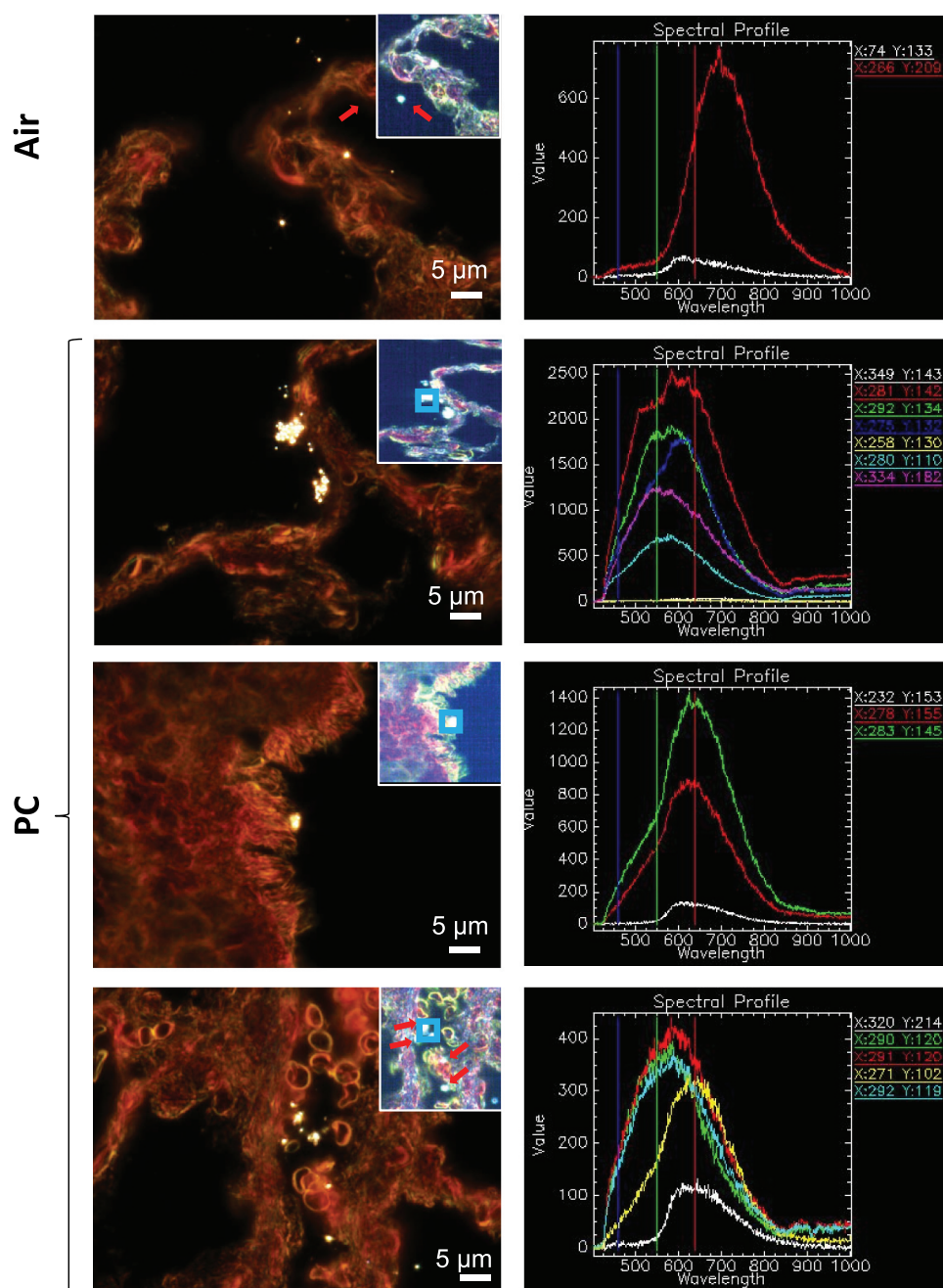


**Figure 8.** Hyperspectral imaging of nanosized particulate in rat lung following 30 days of PC emission exposure. Nanosilica (red arrow) from glass slides was found throughout all X-sections. Suspected PC particles (blue box) were found deposited in alveoli, ciliated airway, and blood vessels.

capillary beds. Few studies have used enhanced darkfield microscopy to identify MNPs in exposed cells and rodent tissue following inhalation exposure (Cary, DeLoid, et al. 2023; Fournier et al. 2020; Moreno et al. 2024; Zhang et al. 2023). Particle agglomerates in this study appeared similar in size and morphology to those nanosized polystyrene beads found in exposed rat placentas via enhanced darkfield microscopy (Cary et al. 2023sa).

Detection and positive identification of deposited PC particles in exposed lung tissues were limited due to our initial inability to collect enough mass of PC UFPs to use as positive identification control for CytoViva, or access to technologies that provide nondestructive nanoscale chemistry identification of plastic particles in tissues. Recent advances in both chemical and physical techniques, including cryogenic laser



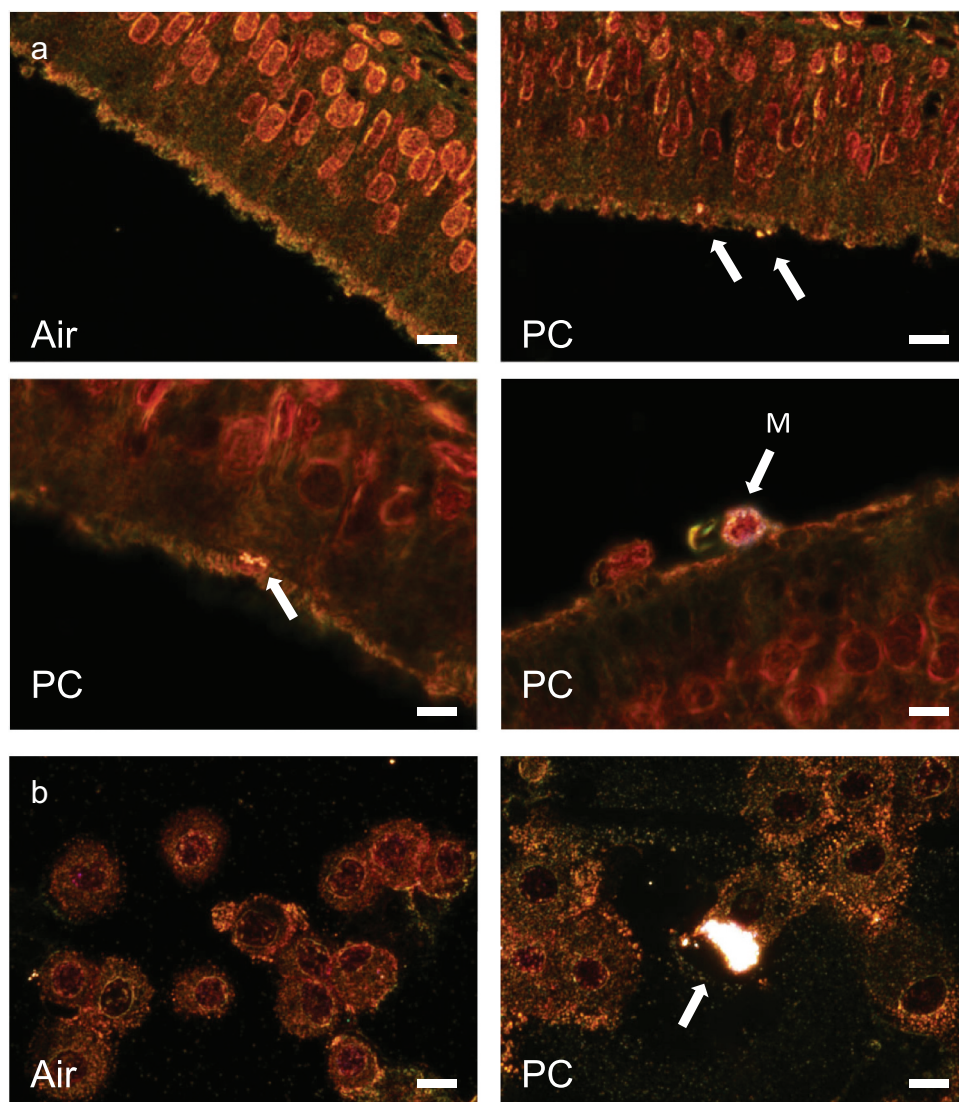


**Figure 9.** Suspected 3D printer PC particle in A) rat nasal epithelium and B) collected BAL cytosin samples after 1 day exposure under enhanced darkfield microscopy. Impacted and deposited suspected PC particle was found as small particle agglomerates on nasal epithelium or occasionally in nasal macrophages (M). Minimal evidence of macrophage uptake of suspected PC agglomerates was observed in BAL cytosin samples. Scale bar is 10  $\mu\text{m}$ .

ablation-assisted mass spectrometry (Wang et al. 2024), hyperspectral stimulated Raman scattering imaging (Qian et al. 2024), and pyrolysis-gas chromatography/mass spectrometry (Campen et al. 2024), might potentially assist with characterizing MNP deposition location, mass, and polymer type in future studies.

Despite the higher exposure concentration and greater estimated lung deposition (248.69  $\mu\text{g}$  vs 60.6  $\mu\text{g}$ ), as reported by M. Farcas et al. (2024), only minimal, transient changes were still observed in all parameters of lung inflammation and toxicity, with no observable changes in histopathology. It is possible to compare these results with our

earlier *in vitro* study by calculating the exposures on a mass per surface area basis. Assuming a total rat alveolar surface area of 4000  $\text{cm}^2$  (Blanco 1992), one can calculate the estimated deposition for the Day 30 group per  $\text{cm}^2$  as 0.0622  $\mu\text{g}$ . In M. T. Farcas et al. (2019), the average deposition of PC particles per  $\text{cm}^2$  of cell culture well was 0.424  $\mu\text{g}/\text{cm}^2$ , an almost 7-fold difference. Thus, it appears that even with the increased aerosol concentration, our current exposure model likely does not reach sufficient deposition levels to elicit an inflammatory response in the lungs.

In general, data on workplace airborne particle mass concentration during FFF 3DP are limited

and results for PC filament specifically are scarce (Dobrzyńska et al. 2021; Min et al. 2021; Stefaniak, Du Preez, and Du Plessis 2021). As such, it is challenging to identify an aerosol mass exposure concentration for inhalation toxicology studies that reflects workplace conditions. For the ABS filament, during the FFF 3DP, particulate matter with diameter less than  $1\text{ }\mu\text{m}$  ( $\text{PM}_{10}$ ) mass concentration in an office was approximately  $0.4\text{ mg/m}^3$  but reached  $2.5\text{ mg/m}^3$  (Katz et al. 2020). For polylactic acid (PLA) filament, total particulate mass concentrations during FFF 3DP in a workroom ranged from  $0.3\text{ mg/m}^3$  when one printer was operated to  $0.7\text{ mg/m}^3$  when three printers were operated at the same time (Chan et al. 2020). For a polyvinyl alcohol (PVA) filament, calculated particulate matter with diameter less than  $2.5\text{ }\mu\text{m}$  ( $\text{PM}_{2.5}$ ) mass concentration in an office reached approximately  $1\text{ mg/m}^3$  (Ding and Ng 2021). In a study that evaluated aerosol mass concentrations during the FFF 3DP with several different filaments (none of which was PC), dust mass levels ranged from  $0.01$  to  $0.03\text{ mg/m}^3$  (Chan et al. 2020; Ding and Ng 2021; Katz et al. 2020; Väisänen et al. 2019). A few studies reported aerosol mass concentrations during the FFF 3DP with PC filament with results ranging from approximately  $1$  to  $4\text{ mg/m}^3$  (Chýlek et al. 2019; McDonnell et al. 2016; Runström et al. 2022). This general range of aerosol mass concentrations reported in the literature for FFF is consistent with the mass exposure concentrations used in our past study ( $0.529\text{ mg/m}^3$ ) (M. Farcas et al. 2024) and the current study ( $2.5\text{ mg/m}^3$ ). At these exposure mass concentrations, only minimal, transient changes were noted in several measures of lung inflammation and toxicity. It is important to recognize that available literature on mass exposure concentrations reflects emissions from one to three FFF 3D printers. Given that aerosol mass emissions increase with the number of FFF 3D printers operating simultaneously (Chan et al. 2020; Karwasz and Osiński 2022), if many printers are operated in a room at the same time, which is common in industry, makerspaces, and academic settings, it is likely that exposure concentrations might exceed  $2.5\text{ mg/m}^3$ . Therefore, evidence of minimal transient effects observed in toxicology studies to date (including the current one) might not be representative of risk for all real-world exposure scenarios.

While this study did not reveal significant pulmonary alterations, previous findings demonstrated that exposure to 3DP FFF emissions might induce systemic effects. For instance, Stefaniak et al. (2017) observed increased blood pressure and impaired vascular function in rats exposed to ABS FFF emissions for a short duration. Our *in vitro* study using human bronchial epithelial cells exposed to real-time ABS FFF emissions reported a significant elevation in pro-inflammatory markers, despite minimal impact on epithelial integrity (M. T. Farcas et al. 2022).

Several studies have highlighted the potential for systemic impacts from inhaled particulate matter. Cary, Seymore, et al. (2023) demonstrated that inhalation of polyamide microplastics led to systemic effects including increased blood pressure and altered reproductive hormones, despite limited pulmonary inflammation (Cary et al. 2024; Cary, Seymore, et al. 2023). Similarly, Tomonaga et al. (2024) observed persistent lung inflammation in rats exposed to polypropylene microplastics, with adverse effects observed at low exposure levels. These findings align with observations following exposure to other nanomaterials, such as  $\text{TiO}_2$  and carbon black (Møller et al. 2016; Tomonaga et al. 2024; van Berlo, Hullmann, and Schins 2012). The mechanisms underlying these extrapulmonary effects might involve both translocation and systemic inflammation. UFPs may translocate from the lungs to other organs via various pathways, including direct passage through the alveolar epithelium (Geiser et al. 2005) and transport along olfactory and trigeminal nerves (Lucchini et al. 2012). Further, UFPs might stimulate the release of inflammatory mediators from the lungs, leading to systemic inflammation and contributing to conditions such as vascular endothelial dysfunction (Helbing et al. 2014; Mandler et al. 2018).

While previous investigators detected VOCs (acetone, benzene, styrene, and toluene) below OSHA permissible exposure limits (PELs) and a BPA concentration of  $21.9 \pm 0.86\text{ }\mu\text{g/m}^3$  (Krajnak et al. 2023), this study, using 5 print heads, measured significantly higher BPA levels ( $78.3 \pm 5.42\text{ }\mu\text{g/m}^3$ ). Although no OSHA PEL exists for BPA, this concentration exceeds recommended European limits ( $0.2\text{ mg/m}^3$  8-hr time-weighted average). Our MPPD-modeled BPA

deposition reached 0.53  $\mu\text{g}/\text{day}$  (1.33  $\mu\text{g}/\text{kg}$  bw/day). These BPA concentrations, comparable to those associated with sexual dysfunction in epoxy resin workers (Hines et al. 2017; Ribeiro, Ladeira, and Viegas 2017), suggest potential physiological relevance of pulmonary BPA deposition from 3DP emissions.

Our prior work demonstrated the inhalation of PC emissions induced neurochemical and hormonal alterations in the olfactory bulb (OB) and hypothalamus, including reduced tyrosine hydroxylase (TH), glial cell line-derived neurotrophic factor (GDNF), myelin basic protein, and cAMP nucleotide phosphatase immunoreactivity (Krajnak et al. 2023). These changes coincided with elevated cell injury markers, reduced mitochondrial activity in the OB, diminished gonadotropin releasing hormone and TH fiber density, decreased spermatogonia, and reduced thyroid stimulating hormone, follicle stimulating hormone, and prolactin levels. These effects may stem from PC particulate/fume interference with olfactory/neuroendocrine function or from BPA, consistent with findings in occupationally exposed populations (Cimmino et al. 2020; Li et al. 2020; Mustieles et al. 2015). Further, our ongoing work (Jackson et al. 2025) indicates that 3DP PC emissions exacerbate asthma in mice, evidenced by increased airway responsiveness, IgE levels, and inflammation. These align with findings linking pre- and post-natal BPA exposure to childhood asthma risk (Wu et al. 2021). BPA's action on estrogen/androgen receptors and its potential to trigger mast cell degranulation and dendritic cell maturation (Bonds and Midoro-Horiuti 2013; Uemura et al. 2008), coupled with our observed increase in TIMP-1, implicated in eosinophilic airway inflammation (Cao et al. 2023), further suggests a connection between 3DP emissions and airway hyperreactivity. Further investigation is needed to fully characterize the mechanisms and health implications of these exposures.

While not a comprehensive evaluation, collectively our findings suggest a strong potential for extra-pulmonary effects (e.g., induction of systemic endocrine, neuronal, and immunological changes) from inhalation of PC thermoplastic

emissions released during 3DP. Outside of the workplace, some of the most common use-cases for 3D printers are in schools and in the home creating the possibility for children and adolescents to be exposed to PC and other 3D printer emissions for many hours of the day, if not properly controlled. Considering the well-documented consequences of BPA exposure on puberty (Leonardi et al. 2017), behavior (Adriani et al. 2003; Mustieles et al. 2015), synapse formation (Leranth et al. 2008), and neurodegenerative diseases (Brown 2009; Golub et al. 2010), reducing or eliminating exposures for these populations is critical. NIOSH has promulgated a guidance document encouraging the use of the hierarchy of controls for reduction of potential FFF exposures, prioritizing elimination, substitution, engineering controls, administrative controls, and personal protective equipment, in that order (Hodson et al. 2023). By following the suggestions provided by this guide, 3D printer users can substantially increase the safety of this technology.

Some important limitations should be noted regarding this study. First, this evaluation used a single type of PC FFF filaments from one manufacturer. FFF filaments vary widely in composition and conclusions drawn from this study need to be limited in scope to a narrow range of similar products. Second, this study only utilized male rats, and it is possible that females may respond differently to this exposure.

## Conclusions

As many as 30 days of inhalation exposure to an occupationally relevant concentration (4 hr/day of 2.5  $\text{mg}/\text{m}^3$ ) of FFF 3DP emissions did not elicit marked inflammatory changes in the rat lung, and some particles appear able to cross the alveolar membrane into circulation. However, there is growing evidence that inhalation of these emissions may alter neuroendocrine function and immune function and care needs to be taken to reduce exposure to these emissions for children and those with respiratory illnesses. The current marketplace contains effectively infinite combinations of proprietary filament types and additives and as such, the findings presented in this study should be understood in that context.



## Disclosure statement

No potential conflict of interest was reported by the author(s).

## Funding

The author(s) reported there is no funding associated with the work featured in this article.

## Data availability statement

The data that support the findings of this study are available from the corresponding author, WKM, upon reasonable request.

## Disclaimer

The findings and conclusions in this report are those of the author(s) and do not necessarily represent the official position of the National Institute for Occupational Safety and Health, Centers for Disease Control and Prevention.

This work has not been reviewed or approved by and may not represent the views of the U.S. Consumer Product Safety Commission. Certain commercial equipment, instruments, or materials are identified in this paper to specify the experimental procedure adequately. Such identification is not intended to imply recommendation or endorsement by the Consumer Product Safety Commission, nor is it intended to imply that the materials or equipment identified are necessarily the best available for the purpose.

## References

- Adriani, W., D. D. Seta, F. Dessi-Fulgheri, F. Farabollini, and G. Laviola. 2003. "Altered Profiles of Spontaneous Novelty Seeking, Impulsive Behavior, and Response to D-Amphetamine in Rats Perinatally Exposed to Bisphenol a." *Environmental Health Perspectives* 111 (4): 395–401. <https://doi.org/10.1289/ehp.5856>.
- Anjilvel, S., and B. Asgharian. 1995. "A Multiple-Path Model of Particle Deposition in the Rat Lung." *Fundamental and Applied Toxicology* 28 (1): 41–50. <https://doi.org/10.1006/faat.1995.1144>.
- Blanco, L. N. 1992. "A Model of Postnatal Formation of Alveoli in Rat Lung." *Journal of Theoretical Biology* 157 (4): 427–446. [https://doi.org/10.1016/S0022-5193\(05\)80662-9](https://doi.org/10.1016/S0022-5193(05)80662-9).
- Bonds, R. S., and T. Midoro-Horiuti. 2013. "Estrogen Effects in Allergy and Asthma." *Current Opinion in Allergy Clinical Immunology* 13 (1): 92–99. <https://doi.org/10.1097/ACI.0b013e32835a6dd6>.
- Brown, J. S., Jr. 2009. "Effects of Bisphenol-A and Other Endocrine Disruptors Compared with Abnormalities of Schizophrenia: An Endocrine-Disruption Theory of Schizophrenia." *Schizophrenia Bulletin* 35 (1): 256–278. <https://doi.org/10.1093/schbul/sbm147>.
- Bus, J. S., S. Su, W. Li, and J. E. Goodman. 2024. "Styrene Lung Cancer Risk Assessment: An Alternative Evaluation of Human Lung Cancer Risk Assuming Mouse Lung Tumors are Potentially Human Relevant and Operating by a Threshold-Based Non-Genotoxic Mode of Action." *Journal of Toxicology and Environmental Health Part B* 27 (7): 264–286. <https://doi.org/10.1080/10937404.2024.2380449>.
- Campen, M., A. Nihart, M. Garcia, R. Liu, M. Olewine, E. Castillo, B. Bleske, et al. 2024. "Bioaccumulation of Microplastics in Decedent Human Brains Assessed by Pyrolysis Gas Chromatography-Mass Spectrometry." *Research Square* 2024.
- Cao, T. B. T., Q. L. Quoc, E. M. Yang, J. Y. Moon, Y. S. Shin, M. S. Ryu, Y. Choi, and H. S. Park. 2023. "Tissue Inhibitor of Metalloproteinase-1 Enhances Eosinophilic Airway Inflammation in Severe Asthma." *Allergy, Asthma & Immunology Research* 15 (4): 451–472. <https://doi.org/10.4168/aaair.2023.15.4.451>.
- Cary, C. M., G. M. DeLoid, Z. Yang, D. Bitounis, M. Polunas, M. J. Goedken, B. Buckley, B. Cheatham, P. A. Stapleton, and P. Demokritou. 2023. "Ingested Polystyrene Nanospheres Translocate to Placenta and Fetal Tissues in Pregnant Rats: Potential Health Implications." *Nanomaterials (Basel)* 13 (4): 720. <https://doi.org/10.3390/nano13040720>.
- Cary, C. M., S. B. Fournier, S. Adams, X. Wang, E. J. Yurkow, and P. A. Stapleton. 2024. "Single Pulmonary Nanopolystyrene Exposure in Late-Stage Pregnancy Dysregulates Maternal and Fetal Cardiovascular Function." *Toxicological Sciences* 199 (1): 149–159. <https://doi.org/10.1093/toxsci/kfae019>.
- Cary, C. M., T. N. Seymore, D. Singh, K. N. Vayas, M. J. Goedken, S. Adams, M. Polunas, et al. 2023. "Single Inhalation Exposure to Polyamide Micro and Nanoplastic Particles Impairs Vascular Dilation without Generating Pulmonary Inflammation in Virgin Female Sprague Dawley Rats." *Particle and Fibre Toxicology* 20 (1): 16. <https://doi.org/10.1186/s12989-023-00525-x>.
- Chan, F. L., C. Y. Hon, S. M. Tarlo, N. Rajaram, and R. House. 2020. "Emissions and Health Risks from the Use of 3D Printers in an Occupational Setting." *Journal of Toxicology and Environmental Health Part A* 83 (7): 279–287. <https://doi.org/10.1080/15287394.2020.1751758>.
- Chýlek, R., L. Kudela, J. Pospíšil, and L. Šnajdárek. 2019. "Fine Particle Emission During Fused Deposition Modelling and Thermogravimetric Analysis for Various Filaments." *Journal of Cleaner Production* 237:117790. <https://doi.org/10.1016/j.jclepro.2019.117790>.
- Cimmino, I., F. Fiory, G. Perruolo, C. Miele, F. Beguinot, P. Formisano, and F. Oriente. 2020. "Potential Mechanisms of Bisphenol a (BPA) Contributing to Human Disease." *International Journal of Molecular Sciences* 21 (16): 5761. <https://doi.org/10.3390/ijms21165761>.

- Cronkite, E. P., R. T. Drew, T. Inoue, Y. Hirabayashi, and J. E. Bullis. 1989. "Hematotoxicity and Carcinogenicity of Inhaled Benzene." *Environmental Health Perspectives* 82:97–108. <https://doi.org/10.1289/ehp.898297>.
- Davis, A. Y., Q. Zhang, J. P. S. Wong, R. J. Weber, and M. S. Black. 2019. "Characterization of Volatile Organic Compound Emissions from Consumer Level Material Extrusion 3D Printers." *Building & Environment* 160:106209. <https://doi.org/10.1016/j.buildenv.2019.106209>.
- Ding, S., and B. F. Ng. 2021. "Particle Emission Levels in the User Operating Environment of Powder, Ink and Filament-Based 3D Printers." *Rapid Prototyping Journal* 27 (6): 1124–1132. <https://doi.org/10.1108/RPJ-02-2020-0039>.
- Dobrzyńska, E., D. Kondej, J. Kowalska, and M. Szewczyńska. 2021. "State of the Art in Additive Manufacturing and Its Possible Chemical and Particle Hazards—Review." *Indoor Air* 31 (6): 1733–1758. <https://doi.org/10.1111/ina.12853>.
- Dunn, K. L., D. Hammond, K. Menchaca, G. Roth, and K. H. Dunn. 2020. "Reducing Ultrafine Particulate Emission from Multiple 3D Printers in an Office Environment Using a Prototype Engineering Control." *Journal of Nanoparticle Research* 22 (5): 1–11. <https://doi.org/10.1007/s11051-020-04844-4>.
- Farcas, M., W. McKinney, W. K. Mandler, A. K. Knepp, L. Battelli, S. A. Friend, A. B. Stefaniak, et al. 2024. "Pulmonary Evaluation of Whole-Body Inhalation Exposure of Polycarbonate (PC) Filament 3D Printer Emissions in Rats." *Journal of Toxicology and Environmental Health Part A* 87 (8): 325–341. <https://doi.org/10.1080/15287394.2024.2311170>.
- Farcas, M. T., W. McKinney, J. Coyle, M. Orandle, W. K. Mandler, A. B. Stefaniak, L. Bowers, et al. 2022. "Evaluation of Pulmonary Effects of 3-D Printer Emissions from Acrylonitrile Butadiene Styrene Using an Air-Liquid Interface Model of Primary Normal Human-Derived Bronchial Epithelial Cells." *International Journal of Toxicology* 41 (4): 312–328. <https://doi.org/10.1177/10915818221093605>.
- Farcas, M. T., W. McKinney, C. Qi, K. W. Mandler, L. Battelli, S. A. Friend, A. B. Stefaniak, et al. 2020. "Pulmonary and Systemic Toxicity in Rats Following Inhalation Exposure of 3-D Printer Emissions from Acrylonitrile Butadiene Styrene (ABS) Filament." *Inhalation Toxicology* 32 (11–12): 403–418. <https://doi.org/10.1080/08958378.2020.1834034>.
- Farcas, M. T., A. B. Stefaniak, A. K. Knepp, L. Bowers, W. K. Mandler, M. Kashon, S. R. Jackson, et al. 2019. "Acrylonitrile Butadiene Styrene (ABS) and Polycarbonate (PC) Filaments Three-Dimensional (3-D) Printer Emissions-Induced Cell Toxicity." *Toxicology Letters* 317:1–12. <https://doi.org/10.1016/j.toxlet.2019.09.013>.
- Feld-Cook, E., and C. P. Weisel. 2021. "Exposure Routes and Types of Exposure." In *Handbook of Indoor Air Quality*, edited by Y. Zhang, P. K. Hopke, and C. Mandin, 1003–1026. Singapore: Springer Singapore.
- Feng, Y., C. Tu, R. Li, D. Wu, J. Yang, Y. Xia, W. Peijnenburg, and Y. Luo. 2023. "A Systematic Review of the Impacts of Exposure to Micro- and Nano-Plastics on Human Tissue Accumulation and Health." *Eco-Environment Health* 2 (4): 195–207. <https://doi.org/10.1016/j.eehl.2023.08.002>.
- Fournier, S. B., J. N. D'Errico, D. S. Adler, S. Kollontzi, M. J. Goedken, L. Fabris, E. J. Yurkow, and P. A. Stapleton. 2020. "Nanopolystyrene Translocation and Fetal Deposition After Acute Lung Exposure During Late-Stage Pregnancy." *Particle and Fibre Toxicology* 17 (1): 55. <https://doi.org/10.1186/s12989-020-00385-9>.
- Geiser, M. 2002. "Morphological Aspects of Particle Uptake by Lung Phagocytes." *Microscopy Research Technique* 57 (6): 512–522. <https://doi.org/10.1002/jemt.10105>.
- Geiser, M., B. Rothen-Rutishauser, N. Kapp, S. Schürch, W. Kreyling, H. Schulz, M. Semmler, V. Im Hof, J. Heyder, and P. Gehr. 2005. "Ultrafine Particles Cross Cellular Membranes by Nonphagocytic Mechanisms in Lungs and in Cultured Cells." *Environmental Health Perspectives* 113 (11): 1555–1560. <https://doi.org/10.1289/ehp.8006>.
- Golub, M. S., K. L. Wu, F. L. Kaufman, L. Li, F. Moran-Messen, L. Zeise, G. V. Alexeeff, and J. M. Donald. 2010. "Bisphenol A: Developmental Toxicity from Early Prenatal Exposure a." *Birth Defects Research Part B, Developmental and Reproductive Toxicology* 89 (6): 441–466. <https://doi.org/10.1002/bdrb.20275>.
- Helbing, T., C. Olivier, C. Bode, M. Moser, and P. Diehl. 2014. "Role of Microparticles in Endothelial Dysfunction and Arterial Hypertension." *World Journal of Cardiology* 6 (11): 1135–1139. <https://doi.org/10.4330/wjc.v6.i11.1135>.
- Hines, C. J., M. V. Jackson, J. A. Deddens, J. C. Clark, X. Ye, A. L. Christianson, J. W. Meadows, and A. M. Calafat. 2017. "Urinary Bisphenol a (BPA) Concentrations Among Workers in Industries That Manufacture and Use BPA in the USA." *Annals of Work Exposures and Health* 61 (2): 164–182. <https://doi.org/10.1093/annweh/wxx021>.
- Hodson, L., K. L. Dunn, K. H. Dunn, E. Glassford, D. Hammond, and G. Roth. 2023. *Approaches to Safe 3D Printing: A Guide for Makerspace Users, Schools, Libraries, and Small Businesses*, edited by C. f. D. C. a. P. DHHS (NIOSH). Cincinnati, OH: U.S. Department of Health and Human Services, National Institute for Occupational Safety and Health.
- Jackson, L., L. Weatherby, W. K. Mandler, W. McKinney, E. Lukomska, M. Cooper, Y. Qian, and S. Anderson. 2025. "Evaluation of Aerosolized 3D Printer Emissions in a Murine Asthma Model." *The Toxicologist* 198 (51): pre-print.
- Karwasz, A., and F. Osinski. 2022. "Analysis of Emission Solid Particles from the 3D Printing Process." *Paper Read at Lecture Notes in Mechanical Engineering*.
- Katz, E. F., J. D. Goetz, C. Wang, J. L. Hart, B. Terranova, M. L. Taheri, M. S. Waring, and P. F. Decarlo. 2020. "Chemical and Physical Characterization of 3D Printer Aerosol Emissions with and without a Filter Attachment."



- Environmental Science & Technology* 54 (2): 947–954. <https://doi.org/10.1021/acs.est.9b04012>.
- Krajnak, K., M. Farcas, W. McKinney, S. Waugh, K. Mandler, A. Knepp, M. Jackson, et al. 2023. "Inhalation of Polycarbonate Emissions Generated During 3D Printing Processes Affects Neuroendocrine Function in Male Rats." *Journal of Toxicology and Environmental Health Part A* 86 (16): 575–596. <https://doi.org/10.1080/15287394.2023.2226198>.
- Kreyling, W. G., S. Hirn, W. Möller, C. Schleh, A. Wenk, G. Celik, J. Lipka, et al. 2014. "Air–Blood Barrier Translocation of Tracheally Instilled Gold Nanoparticles Inversely Depends on Particle Size." *ACS Nano Journal* 8 (1): 222–233. <https://doi.org/10.1021/nn403256v>.
- Leonardi, A., M. Cofini, D. Rigante, L. Lucchetti, C. Cipolla, L. Penta, and S. Esposito. 2017. "The Effect of Bisphenol a on Puberty: A Critical Review of the Medical Literature." *International Journal of Environmental Research and Public Health* 14 (9): 1–22. <https://doi.org/10.3390/ijerph14091044>.
- Leranth, C., T. Hajszan, K. Szigeti-Buck, J. Bober, and N. J. MacLusky. "Bisphenol a Prevents the Synaptogenic Response to Estradiol in Hippocampus and Prefrontal Cortex of Ovariectomized Nonhuman Primates." *Proceedings of the National Academy of Sciences of the USA* 105 (37): 14187–14191. 2008 Sep 16. [10.1073/pnas.0806139105](https://doi.org/10.1073/pnas.0806139105).
- Li, X., Z. Wen, Y. Wang, J. Mo, Y. Zhong, and R. Ge. 2020. "Bisphenols and Leydig Cell Development and Function." *Frontiers in Endocrinology* 11:447. <https://doi.org/10.3389/fendo.2020.00447>.
- Liao, C., C. Chio, W. Chen, Y. Ju, W. Li, Y. Cheng, V. H. Liao, S. C. Chen, and M. P. Ling. 2011. "Lung Cancer Risk in Relation to Traffic-Related Nano/Ultrafine Particle-Bound PAHs Exposure: A Preliminary Probabilistic Assessment." *Journal of Hazardous Materials* 190 (1–3): 150–158. <https://doi.org/10.1016/j.jhazmat.2011.03.017>.
- Lucchini, R. G., D. C. Dorman, A. Elder, and B. Veronesi. 2012. "Neurological Impacts from Inhalation of Pollutants and the Nose–Brain Connection." *Neurotoxicology* 33 (4): 838–841. <https://doi.org/10.1016/j.neuro.2011.12.001>.
- MacNee, W., and K. Donaldson. 2003. "Mechanism of Lung Injury Caused by PM<sub>10</sub> and Ultrafine Particles with Special Reference to COPD." *The European Respiratory Journal* 21 (40 suppl): 47s–51s. <https://doi.org/10.1183/09031936.03.00403203>.
- Mandler, W. K., T. R. Nurkiewicz, D. W. Porter, E. E. Kelley, and I. M. Olfert. 2018. "Microvascular Dysfunction Following Multiwalled Carbon Nanotube Exposure is Mediated by Thrombospondin-1 Receptor CD47." *Toxicological Sciences* 165 (1): 90–99. <https://doi.org/10.1093/toxsci/kfy120>.
- Mandler, W. K., T. R. Nurkiewicz, D. W. Porter, and I. M. Olfert. 2017. "Thrombospondin-1 Mediates Multi-Walled Carbon Nanotube Induced Impairment of Arteriolar Dilation." *Nanotoxicology* 11 (1): 112–122. <https://doi.org/10.1080/17435390.2016.1277275>.
- McDonnell, B., X. J. Guzman, M. Dolack, T. W. Simpson, and J. M. Cimbala. 2016. "3D Printing in the Wild: A Preliminary Investigation of Air Quality in College Maker Spaces." *Paper read at Solid Freeform Fabrication 2016: Proceedings of the 27th Annual International Solid Freeform Fabrication Symposium - An Additive Manufacturing Conference, SFF 2016*. Austin, Texas.
- Min, K., Y. Li, D. Wang, B. Chen, M. Ma, L. Hu, Q. Liu, and G. Jiang. 2021. "3D Printing-Induced Fine Particle and Volatile Organic Compound Emission: An Emerging Health Risk." *Environmental Science & Technology Letters* 8 (8): 616–625. <https://doi.org/10.1021/acs.estlett.1c00311>.
- Møller, P., D. V. Christophersen, N. R. Jacobsen, A. Skovmand, A. C. Gouveia, M. H. Andersen, A. Kermanizadeh, et al. 2016. "Atherosclerosis and Vasomotor Dysfunction in Arteries of Animals After Exposure to Combustion-Derived Particulate Matter or Nanomaterials." *Critical Reviews in Toxicology* 46 (5): 437–476. <https://doi.org/10.3109/10408444.2016.1149451>.
- Moreno, G. M., T. Brunson-Malone, S. Adams, C. Nguyen, T. N. Seymore, C. M. Cary, M. Polunas, M. J. Goedken, and P. A. Stapleton. 2024. "Identification of Micro- and Nanoplastic Particles in Postnatal Sprague-Dawley Rat Offspring After Maternal Inhalation Exposure Throughout Gestation." *Science of the Total Environment* 951:175350. <https://doi.org/10.1016/j.scitotenv.2024.175350>.
- Mustieles, V., R. Pérez-Lobato, N. Olea, and M. F. Fernandez. 2015. "Bisphenol A: Human Exposure and Neurobehavior." *Neurotoxicology* 49:174–184. <https://doi.org/10.1016/j.neuro.2015.06.002>.
- Nemmar, A., P. H. Hoet, B. Vanquickenborne, D. Dinsdale, M. Thomeer, M. F. Hoylaerts, H. Vanbilloen, L. Mortelmans, and B. Nemery. 2002. "Passage of Inhaled Particles into the Blood Circulation in Humans." *Circulation* 105 (4): 411–414. <https://doi.org/10.1161/hc0402.104118>.
- Oberdörster, G. 2000. "Pulmonary Effects of Inhaled Ultrafine Particles." *International Archives of Occupational and Environmental Health* 74 (1): 1–8. <https://doi.org/10.1007/s004200000185>.
- Occupational, Safety, Administration Health, and Daren Pearce. "OSHA Method 1018, Bisphenol A, Diglycidyl Ether of Bisphenol a."
- Occupational, Safety, Administration Health, and Kevin Cummins. "OSHA Method 32, Phenol and Cresol."
- Peters, A., H. E. Wichmann, T. Tuch, J. Heinrich, and J. Heyder. 1997. "Respiratory Effects are Associated with the Number of Ultrafine Particles." *American Journal of Respiratory and Critical Care Medicine* 155 (4): 1376–1383. <https://doi.org/10.1164/ajrccm.155.4.9105082>.
- Placek, M. P. 2023. *Additive Manufacturing and 3D Printing - Statistics & Facts*, Statista. Accessed May 25, 23. <https://www.statista.com/topics/1969/additive-manufacturing-and-3d-printing/#topicOverview>.
- Qian, N., X. Gao, X. Lang, H. Deng, T. M. Bratu, Q. Chen, P. Stapleton, B. Yan, and W. Min. 2024. "Rapid

- Single-Particle Chemical Imaging of Nanoplastics by SRS Microscopy.” *Proceedings of the National Academy of Sciences* 121 (3): e2300582121. <https://doi.org/10.1073/pnas.2300582121>.
- Ribeiro, E., C. Ladeira, and S. Viegas. 2017. “Occupational Exposure to Bisphenol a (BPA): A Reality That Still Needs to Be Unveiled.” *Toxics* 5 (3): 22. <https://doi.org/10.3390/toxics5030022>.
- Runström, E. G., H. Tinnerberg, L. Rosell, R. Möller, A. C. Almstrand, and A. Bredberg. 2022. “Exploring Methods for Surveillance of Occupational Exposure from Additive Manufacturing in Four Different Industrial Facilities.” *Annals of Work Exposures and Health* 66 (2): 163–177. <https://doi.org/10.1093/annweh/wxab070>.
- Stefaniak, A. B., S. Du Preez, and J. L. Du Plessis. 2021. “Additive Manufacturing for Occupational Hygiene: A Comprehensive Review of Processes, Emissions, and Exposures.” *Journal of Toxicology and Environmental Health Part B* 24 (5): 173–222. <https://doi.org/10.1080/10937404.2021.1936319>.
- Stefaniak, A. B., A. R. Johnson, S. du Preez, D. R. Hammond, J. R. Wells, J. E. Ham, R. F. LeBouf, et al. 2019. “Evaluation of Emissions and Exposures at Workplaces Using Desktop 3-Dimensional Printers.” *Journal of Chemical Health and Safety* 26 (2): 19–30. <https://doi.org/10.1016/j.jchas.2018.11.001>.
- Stefaniak, A. B., R. F. LeBouf, M. G. Duling, J. Yi, A. B. Abukabda, C. R. McBride, and T. R. Nurkiewicz. 2017. “Inhalation Exposure to Three-Dimensional Printer Emissions Stimulates Acute Hypertension and Microvascular Dysfunction.” *Toxicology & Applied Pharmacology* 335:1–5. <https://doi.org/10.1016/j.taap.2017.09.016>.
- Stueckle, T. A., D. C. Davidson, R. Derk, T. G. Kornberg, L. Battelli, S. Friend, M. Orandle, et al. 2018. “Short-Term Pulmonary Toxicity Assessment of Pre- and Post-Incinerated Organomodified Nanoclay in Mice.” *ACS Nano Journal* 12 (3): 2292–2310. <https://doi.org/10.1021/acsnano.7b07281>.
- Swenberg, J. A., B. C. Moeller, K. Lu, J. E. Rager, R. C. Fry, and T. B. Starr. 2013. “Formaldehyde Carcinogenicity research: 30 Years and Counting for Mode of Action, epidemiology, and Cancer Risk Assessment.” *Toxicologic Pathology* 41 (2): 181–189. <https://doi.org/10.1177/0192623312466459>.
- Tedla, G., A. M. Jarabek, P. Byrley, W. Boyes, and K. Rogers. 2022. “Human Exposure to Metals in Consumer-Focused Fused Filament Fabrication (FFF)/3D Printing Processes.” *Science of the Total Environment* 814:152622. <https://doi.org/10.1016/j.scitotenv.2021.152622>.
- Tedla, G., and K. Rogers. 2023. “Characterization of 3D Printing Filaments Containing Metal Additives and Their Particulate Emissions.” *Science of the Total Environment* 875:162648. <https://doi.org/10.1016/j.scitotenv.2023.162648>.
- Tomonaga, T., H. Higashi, H. Izumi, C. Nishida, N. Kawai, K. Sato, T. Morimoto, Y. Higashi, K. Yatera, and Y. Morimoto. 2024. “Investigation of Pulmonary Inflammatory Responses Following Intratracheal Instillation of and Inhalation Exposure to Polypropylene Microplastics.” *Particle and Fibre Toxicology* 21 (1): 29. <https://doi.org/10.1186/s12989-024-00592-8>.
- Uemura, Y., T. Y. Liu, Y. Narita, M. Suzuki, and S. Matsushita. 2008. “17 $\beta$ -Estradiol (E2) Plus Tumor Necrosis Factor- $\alpha$  Induces a Distorted Maturation of Human Monocyte-Derived Dendritic Cells and Promotes Their Capacity to Initiate T-Helper 2 Responses.” *Human Immunology* 69 (3): 149–157. <https://doi.org/10.1016/j.humimm.2008.01.017>.
- Väisänen, A. J. K., M. Hyttinen, S. Ylönen, and L. Alonen. 2019. “Occupational Exposure to Gaseous and Particulate Contaminants Originating from Additive Manufacturing of Liquid, Powdered, and Filament Plastic Materials and Related Post-Processes.” *Journal of Occupational and Environmental Hygiene* 16 (3): 258–271. <https://doi.org/10.1080/15459624.2018.1557784>.
- van Berlo, D., M. Hullmann, and R. P. Schins. 2012. “Toxicology of Ambient Particulate Matter.” *Experientia Supplementum* 101:165–217. doi:10.1007/978-3-7643-8340-4\_7.
- Wang, Y., J. J. Bai, Y. J. Wei, C. X. Zhao, Z. Shao, M. L. Chen, and J. H. Wang. 2024. “Tracking and Imaging Nano-Plastics in Fresh Plant Using Cryogenic Laser Ablation Inductively Coupled Plasma Mass Spectrometry.” *Journal of Hazardous Materials* 465:133029. <https://doi.org/10.1016/j.jhazmat.2023.133029>.
- Wu, M., S. Wang, Q. Weng, H. Chen, J. Shen, Z. Li, Y. Wu, et al. 2021. “Prenatal and Postnatal Exposure to Bisphenol a and Asthma: A Systemic Review and Meta-Analysis.” *Journal of Thoracic Diseases* 13 (3): 1684–1696. <https://doi.org/10.21037/jtd-20-1550>.
- Yi, J., R. F. LeBouf, M. G. Duling, T. Nurkiewicz, B. T. Chen, D. Schwegler-Berry, M. A. Virji, and A. B. Stefaniak. 2016. “Emission of Particulate Matter from a Desktop Three-Dimensional (3D) Printer.” *Journal of Toxicology and Environmental Health Part A* 79 (11): 453–465. <https://doi.org/10.1080/15287394.2016.1166467>.
- Young, J. T. 1981. “Histopathologic Examination of the Rat Nasal Cavity.” *Fundamental and Applied Toxicology* 1 (4): 309–312. [https://doi.org/10.1016/S0272-0590\(81\)80037-1](https://doi.org/10.1016/S0272-0590(81)80037-1).
- Zárybnická, L., R. Ševčík, J. Pokorný, D. Machová, E. Stránská, and J. Šál. 2022. “CaCO(3) Polymorphs Used as Additives in Filament Production for 3D Printing.” *Polymers (Basel)* 14 (1): 199. <https://doi.org/10.3390/polym14010199>.
- Zhang, H. J., H. R. Zhou, W. Pan, C. Wang, Y. Y. Liu, L. Yang, M. Tsz-Ki Tsui, and A. J. Miao. 2023. “Accumulation of Nanoplastics in Human Cells as Visualized and Quantified by Hyperspectral Imaging with Enhanced Dark-Field Microscopy.” *Environment International* 179:108134. <https://doi.org/10.1016/j.envint.2023.108134>.